

## Evaluation of color removal efficiencies and kinetic parameters of Fenton ( $H_2O_2/Fe^{2+}$ ) and photo-Fenton ( $H_2O_2/Fe^{2+}/UV$ ) processes in the treatment of a textile wastewater containing indigo blue

### Avaliação da eficiência de remoção de cor e parâmetros cinéticos dos processos de Fenton ( $H_2O_2/Fe^{2+}$ ) e foto-Fenton ( $H_2O_2/Fe^{2+}/UV$ ) no tratamento de um efluente têxtil contendo corante azul índigo

DOI:10.34117/bjdv7n11-044

Recebimento dos originais: 10/10/2021

Aceitação para publicação: 04/11/2021

#### Jean Cesar Benassi

Mestre em Ciências – Programa: Têxtil e Moda - EACH/USP - School of Arts - Sciences and Humanities - Textile and Fashion Course - University of São Paulo  
Av. Arlindo Béttio, 1000 - Parque Ecológico do Tietê - Ermelino Matarazzo - São Paulo - SP  
E-mail: quimicojean@gmail.com

#### Annie Alexandra Cerón Sánchez

Ph.D em Ciências - Programa: Biotecnologia Industrial EEL/USP  
School of Arts, Sciences and Humanities, Textile and Fashion Course, University of São Paulo  
Av. Arlindo Béttio, 1000 - Parque Ecológico do Tietê - Ermelino Matarazzo - São Paulo - SP  
E-mail: acerons@usp.br

#### Silgia Aparecida da Costa

<https://orcid.org/0000-0001-8331-538X>  
Ph.D Engenharia Têxtil UMINHO/Portugal - School of Arts - Sciences and Humanities - Textile and Fashion Course - University of São Paulo  
Av. Arlindo Béttio, 1000 - Parque Ecológico do Tietê - Ermelino Matarazzo - São Paulo - SP  
E-mail: silgia@usp.br

#### Sirlene Maria da Costa

Ph.D Biotecnologia Industrial FAENQUIL atual EEL/USP - School of Arts Sciences and Humanities - Textile and Fashion Course - University of São Paulo  
Av. Arlindo Béttio, 1000 - Parque Ecológico do Tietê - Ermelino Matarazzo - São Paulo - SP  
E-mail: sirlene@usp.br

#### ABSTRACT

The textile industry uses Indigo blue dye extensively in the production of jeans. Thus, high volumes of wastewater containing dye are obtained and must be treated before being discharged. The color removal efficiencies of indigo blue dye synthetic wastewater after treatment by Advanced Oxidative Processes (AOPs) using Fenton ( $H_2O_2/Fe^{2+}$ ) and photo-Fenton ( $H_2O_2/Fe^{2+}/UV$ ) was evaluated in this work. The experiments were conducted at pH 2.8 and evaluated the influence of the amount of  $[H_2O_2]/[Fe^{2+}]$ , the use of sulfuric acid and citric acid to adjust the pH, the initial concentration of the indigo dye, and the dosage form of  $H_2O_2$  - the kinetic parameters and BMG model were also evaluated. The use of sulfuric acid to adjust the pH was more efficient in removing the color. The highest color removal rates were  $70.78 \pm 2.96$  % after 180 min and  $64.22 \pm 2.08$  % after 60 min, respectively, for the Fenton and photo-Fenton

processes (both with a single dose of reagents) and  $79.76 \pm 1.45$  % after 300 min and  $80.43 \pm 1.27$ % after 180 min, respectively, for Fenton and photo-Fenton with the gradual addition of  $H_2O_2$ . The indigo dye degradation reactions are better suited to the BMG kinetic model.

**Keywords:** Indigo blue dye, Textile wastewater, Advanced Oxidative Processes, Fenton process, Color removal.

## RESUMO

A indústria têxtil utiliza extensivamente o corante azul índigo na produção de jeans. Assim, são obtidos grandes volumes de águas residuais contendo corante, que devem ser tratadas antes de serem descarregadas. A eficiência da remoção de cor das águas residuais sintéticas do corante azul índigo após tratamento por Processos Oxidativos Avançados (AOPs) usando Fenton ( $H_2O_2/Fe^{2+}$ ) e foto-Fenton ( $H_2O_2/Fe^{2+}/UV$ ) foi avaliada neste trabalho. As experiências foram realizadas a pH 2,8 e avaliou-se a influência da quantidade de  $[H_2O_2]/[Fe^{2+}]$ , o uso de ácido sulfúrico e ácido cítrico para ajustar o pH, a concentração inicial do corante índigo, e a forma de dosagem de  $H_2O_2$  - os parâmetros cinéticos e o modelo BMG também foram avaliados. A utilização de ácido sulfúrico para ajustar o pH foi mais eficiente na remoção da cor. As maiores taxas de remoção da cor foram  $70,78 \pm 2,96$ % após 180 min e  $64,22 \pm 2,08$ % após 60 min, respectivamente, para os processos Fenton e foto-Fenton (ambos com uma dose única de reagentes) e  $79,76 \pm 1,45$ % após 300 min e  $80,43 \pm 1,27$ % após 180 min, respectivamente, para Fenton e foto-Fenton com a adição gradual de  $H_2O_2$ . As reações de degradação do corante índigo são mais adequadas para o modelo cinético BMG.

**Palavras-chave:** Corante azul índigo, Águas residuais têxteis, Processos oxidativos avançados, processo Fenton, Remoção de cor.

## 1 INTRODUCTION

In recent years, Advanced Oxidative Processes (AOP) have attracted the interest of researchers, as they are considered a viable option for difficult-to-remove organic pollutants from industrial wastewater (Kumar, Singh and Shah, 2021; Mahtab, Farooqi and Khursheed, 2021; Ramos et al., 2021). In addition, the material has the advantage of removing the color from the effluents and not transferring pollutants from one phase to another as in conventional treatments, nor producing large amounts of hazardous sludge, which is why these processes have been used in the most diverse industrial fields (Mishra et al., 2017).

The AOPs processes consist of the generation of the hydroxyl radical ( $\bullet OH$ ), which is the main responsible for the oxidation of organic matter. The free  $\bullet OH$  radical has a highest oxidizing potential (2.8 eV), which accelerate the oxidation and degradation of a wide range of contaminants in wastewater (Khatri, Singh and Garg, 2018; Kumar, Singh and Shah, 2021; Lima et al., 2021).

According to the AOP used, hydroxyl radicals can be achieved by means of several processes. Chemical oxidation using hydrogen peroxide ( $H_2O_2$ ), ozone ( $O_3$ ), hydrogen peroxide/ozone ( $H_2O_2/O_3$ ), Fenton's reagent; radiation methods, such as ultraviolet (UV)

radiation, gamma radiation, electron beam, and ultrasonic waves (sonolysis). Other processes are a joint application of the chemical and radiation methods, such as UV radiation or ultrasound; and photocatalysis using UV radiation and titanium dioxide (TiO<sub>2</sub>) (Kumar, Singh and Shah, 2021; Ramos et al., 2021).

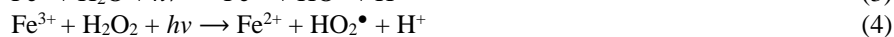
Among the AOPs treatments, the Fenton process represents an attractive option for the treatment of effluents, because it presents a low risk to human and environmental health and because its application doesn't require complex equipment and extreme operating conditions (Ou et al., 2013).

Fenton's process consists of the reaction between Fe<sup>2+</sup> and H<sub>2</sub>O<sub>2</sub> to produce the hydroxyl radical •OH (Eq. 1). Furthermore, iron may initially be in the form of Fe<sup>2+</sup> or Fe<sup>3+</sup> because the reaction of Fe<sup>3+</sup> with H<sub>2</sub>O<sub>2</sub> regenerates Fe<sup>2+</sup> (Eq. 2) (Miller, Wadley and Waite, 2017).

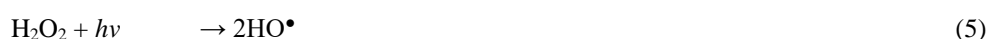


The conventional Fenton process is only efficient in the pH 2-4 range and is generally most efficient around pH 2.8. Therefore, in the pH range of most natural waters the process is inefficient. This is particularly due to the tendency of precipitation of Fe(OH)<sub>3</sub> (which has low catalytic activity), which tends to occur at pH greater than 3-4, depending on the iron concentration (Babuponnusami and Muthukumar, 2014).

When UV light (180-400 nm) is applied in combination with H<sub>2</sub>O<sub>2</sub> and Fe<sup>3+</sup> this causes the formation of •OH hydroxyl radicals causing the reduction of Fe<sup>3+</sup> to Fe<sup>2+</sup> (Eq. 3 and Eq. 4), this reaction is called photo-Fenton. Now the regenerated Fe<sup>2+</sup> can start a new reaction cycle (Miller, Wadley and Waite, 2017; Ameta et al., 2018).



Irradiation of UV light on H<sub>2</sub>O<sub>2</sub> also leads to the formation of •OH, increasing the efficiency of the treatment (Eq. 5) (Hafezi et al., 2020).



Thus, it is expected a greater generation of •OH radicals by the action of UV light in the photo-Fenton process, causing a greater amount of organic matter to be degraded in a shorter period (Yu et al., 2020).

However, excess hydrogen peroxide or high concentrations of  $\bullet\text{OH}$  can lead to parallel reactions resulting in the elimination of  $\bullet\text{OH}$  or the formation of a lower oxidizing radical  $\text{HO}_2\bullet$  (Eq. 6 to 10), decreasing the degradation reaction of the organic matter (Mirzaei et al., 2017).



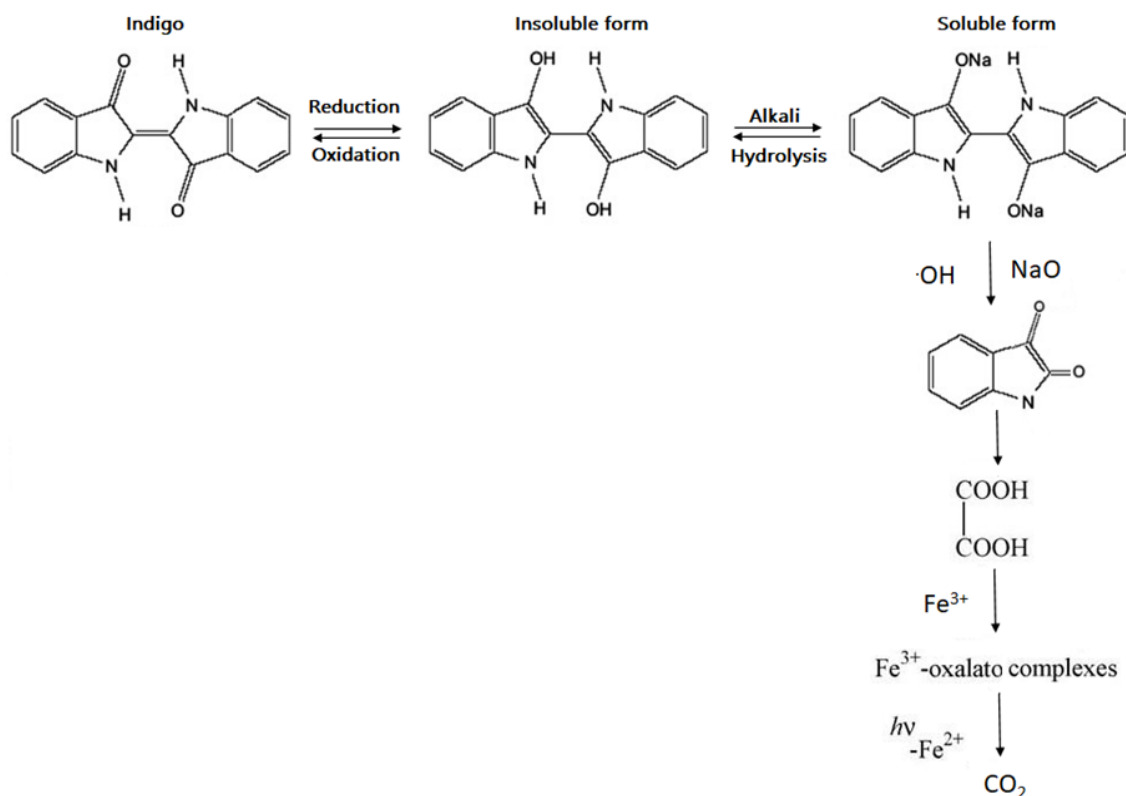
The important factors that can influence color removal in Fenton and photo-Fenton treatments are dye and reagents concentrations, presence of other organic pollutants, type of catalyst, treatment time, UV radiation intensity (photo-Fenton), pH, chemical structure of dyes and dyeing auxiliaries, water quality, effluent salinity, temperature, and reagent feeding mode (Babuponnusami and Muthukumar, 2014; Mirzaei et al., 2017; Zhang et al., 2019; Hafezi et al., 2020).

Fenton and photo-Fenton processes also have the advantage of being able to treat effluents containing soluble and insoluble dyes (Katheresan, Kansedo and Lau, 2018), as in the case of indigo dye, which has very low solubility in water (Chowdhury et al., 2020).

Advanced Oxidation Processes have been more frequently studied for the indigo carmine dye (Palma-Goyes et al., 2014, 2018; Saggiaro et al., 2015; Garcia et al., 2017; Zukawa et al., 2019; Chowdhury et al., 2020; Ramos et al., 2020; Zhao et al., 2020). Few works involving AOPs have been published for indigo blue so far, mainly by Fenton process (Hendaoui et al., 2018). Vedrenne et al., 2012, for example, carried out a study for the treatment of wastewater containing indigo blue by a photo-Fenton process mediated by ferrous oxalate. The results were satisfactory in the removal of Total Organic Carbon (TOC) but did not present effects related to the color removal rate. According to (Chowdhury et al., 2020), this dye has high stability and complex structure, which hinders its biological degradation, and POA processes, which, when used as a pre-treatment, can produce an effluent that can be biodegraded (Vedrenne et al., 2012).

Indigo blue ( $\text{C}_{16}\text{H}_{10}\text{N}_2\text{O}_2$ ) is a synthetic organic dye insoluble in aqueous solutions. For the dyeing process it needs to be reduced to its leuco form (soluble form) using a strong reducing agent in alkaline solution (pH 11 to 14). The leuco form has a chemical affinity with cellulose (Amaral et al., 2014; Mishra et al., 2017; Nature, 2021). Fig. 1 shows the oxidation/reduction mechanism, and the Fenton indigo blue degradation.

Fig. 1. General reaction sequence proposed for the degradation of indigo blue by-Fenton assisted photon. Adapted from (Amaral et al., 2014; Nature, 2021)



The annual production of indigo dye is approximately 50,000 tons (Mahakulkar et al., 2019). It is widely used in the dyeing of denim, as it gives jeans its characteristic blue color. Although indigo has poor colorfastness to wash, this aspect is considered an advantage in achieving the desired look and design. Although considered an advantage, this can lead to effluent problems during the dyeing and washing processes of denim clothes (Paul, 2015). In addition, denim production and dyeing processes with indigo dye consume an excessive volume of water (Garcia, 2015; Yukseler et al., 2017).

It is estimated that 5 to 20% of the dye is lost during the dyeing of the textile fibers. This is a direct result from the lack of complete fixation, having as destination the disposal as a residual effluent that ends up being dumped in rivers and streams, causing several environmental problems, if not properly addressed before final disposal (Dojčinović et al., 2011; Ghazi Mokri et al., 2015; Kalra and Gupta, 2019).

In this work, an evaluation of color removal and kinetic parameters of textile wastewater containing indigo blue dye treated by Fenton (H<sub>2</sub>O<sub>2</sub>/Fe<sup>2+</sup>) and photo-Fenton (H<sub>2</sub>O<sub>2</sub>/Fe<sup>2+</sup>/UV) processes was performed.

## 2 MATERIALS AND METHODS

### 2.1. MATERIALS

Indigo Blue synthetic dye (dark blue powder, 262.26 molecular weight and relative density of  $1.35 \text{ g/cm}^3$  at  $20 \text{ }^\circ\text{C}$ ) was provided by Quimanil Produtos Químicos Ltda, iron sulfate heptahydrate ( $\text{Fe}_2\text{SO}_4 \cdot 7\text{H}_2\text{O}$ ), 98% sulfuric acid ( $\text{H}_2\text{SO}_4$ ), sodium hydrosulfite ( $\text{Na}_2\text{S}_2\text{O}_4$ ) and sodium hydroxide ( $\text{NaOH}$ ) were acquired from the company Nox Solutions; 50% hydrogen peroxide ( $\text{H}_2\text{O}_2$ ) and citric acid ( $\text{C}_6\text{H}_8\text{O}_7$ ) were provided by the company Labsynth. The catalase Goldzime HPX- enzymatic activity  $\geq 19,000.0 \text{ CIU / mL}$  was provided by Golden Technology do Brazil.

### 2.2 SYNTHETIC WASTEWATER

Synthetic wastewater was prepared in the laboratory from a dye stock solution containing indigo at  $2 \text{ g L}^{-1}$  of dye,  $1.26 \text{ g L}^{-1}$  of sodium hydroxide and  $1.54 \text{ g L}^{-1}$  of sodium hydrosulfite. This solution was prepared based on the concentration range of 1 to  $4 \text{ g L}^{-1}$  used in indigo dyeing by textile industries (Meksi and Mhenni, 2015).

To conduct the studies using Fenton and photo-Fenton, wastewater was prepared at concentrations of 0.1, 0.2, 0.4, and 0.8 of indigo  $\text{g L}^{-1}$ , diluting the stock solution.

### 2.3 WASTEWATER TREATMENT WITH FENTON AND PHOTO-FENTON

Fenton processes were carried out in a 1000 ml beaker containing 500 ml of the synthetic wastewater solution. The beaker was placed on a stir plate and, to maintain in magnetic stirring at 200 rpm during the treatment. The experiments were conducted at  $22 \text{ }^\circ\text{C}$ .

The processes were performed using iron (II) sulfate heptahydrate ( $\text{FeSO}_4 \cdot 7\text{H}_2\text{O}$ ) as a source of  $\text{Fe}^{2+}$  ions and hydrogen peroxide ( $\text{H}_2\text{O}_2$ ) 50 %. To verify the influence of the type of acid, sulfuric acid  $0.5 \text{ mol L}^{-1}$ , and citric acid  $300 \text{ g L}^{-1}$  were used to adjust the pH to 2.8. As reported by other authors, Fenton processes are more efficient between a pH range of 2.5 and 3.0 (Qiu and Huang, 2010; Miller, Wadley and Waite, 2017; Nicodemos Ramos, Sousa and Aguiar, 2020).

Treatments by photo-Fenton were carried out in the same way that Fenton. In this case, the beaker containing the synthetic solution of wastewater was taken to the photochemical reactor as shown in Fig. 2. It has a source of polychromatic UV/Visible radiation, which is ensured by 3 lamps with a maximum emission between 253.1 nm and 320.0 nm and power to emit 1.7 Watts/UV and an average lifetime of approximately 6000 hours. The reactor consists of a wooden

chamber that has been internally coated with aluminum foil to ensure that all radiation was reflected on the sample.

The reactor was also equipped with a cooler, used to keep the temperature controlled – in a climate-controlled laboratory, it remained in the range of 22 °C inside the chamber throughout the experiment. The reactor has an opening at the bottom that allows the coupling of a magnetic stirring plate to maintain a constant agitation of 200 rpm during the experiments.

Fig. 2. Schematic representation of the reactor used for the treatment synthetic wastewater. (a) Wooden chamber, (b) door, (c) on-off switch, (d) UV lamp, (e) cooler, (f) Beaker with sample and (g) magnetic stirrer

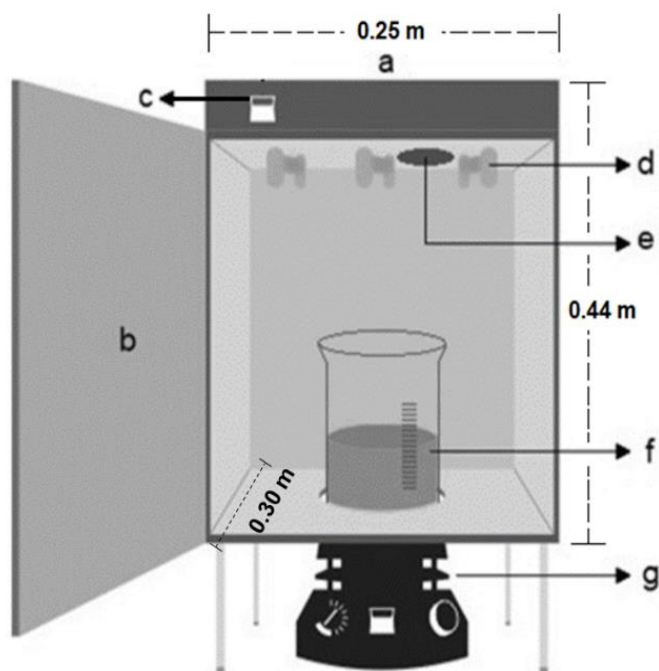


Table 1 presents the experimental conditions of the treatments of synthetic wastewater containing indigo performed by Fenton and photo-Fenton.

To evaluate the effect of the initial concentration of  $[H_2O_2]: [Fe^{2+}]$ , experiments were carried out increasing the amounts of  $H_2O_2$  and  $Fe^{2+}$  added but keeping the ratio of 20:1 (m/m) (experiments 1 to 10) for Fenton and (experiments 15 to 24) for photo-Fenton). Studies have reported that an optimal ratio of  $H_2O_2$  and  $Fe^{2+}$  in Fenton and photo-Fenton treatments ranges between 10:1 and 25:1 (Palma-Goyes et al., 2014).

Table 1. Experimental conditions of the Fenton and photo-Fenton processes for the treatment of synthetic wastewater prepared in a volume of 500ml

Experiments	Method	Acid used	Dosage of H <sub>2</sub> O <sub>2</sub>	[indigo] (g L <sup>-1</sup> )	[Fe <sup>2+</sup> ] (mg L <sup>-1</sup> )	[H <sub>2</sub> O <sub>2</sub> ] (mg L <sup>-1</sup> )
1	Fenton	Sulfuric	Single	0.2	25.0	0500
2	Fenton	Sulfuric	Single	0.2	37.5	0750
3	Fenton	Sulfuric	Single	0.2	50.0	1000
4	Fenton	Sulfuric	Single	0.2	62.5	1250
5	Fenton	Sulfuric	Single	0.2	75.0	1500
6	Fenton	Citric	Single	0.2	25.0	0500
7	Fenton	Citric	Single	0.2	37.5	0750
8	Fenton	Citric	Single	0.2	50.0	1000
9	Fenton	Citric	Single	0.2	62.5	1250
10	Fenton	Citric	Single	0.2	75.0	1500
11	Fenton	Sulfuric	Gradual	0.1	75.0	*
12	Fenton	Sulfuric	Gradual	0.2	75.0	*
13	Fenton	Sulfuric	Gradual	0.4	75.0	*
14	Fenton	Sulfuric	Gradual	0.8	75.0	*
15	photo-Fenton	Sulfuric	Single	0.2	25.0	0500
16	photo-Fenton	Sulfuric	Single	0.2	37.5	0750
17	photo-Fenton	Sulfuric	Single	0.2	50.0	1000
18	photo-Fenton	Sulfuric	Single	0.2	62.5	1250
19	photo-Fenton	Sulfuric	Single	0.2	75.0	1500
20	photo-Fenton	Citric	Single	0.2	25.0	0500
21	photo-Fenton	Citric	Single	0.2	37.5	0750
22	photo-Fenton	Citric	Single	0.2	50.0	1000
23	photo-Fenton	Citric	Single	0.2	62.5	1250
24	photo-Fenton	Citric	Single	0.2	75.0	1500
25	photo-Fenton	Sulfuric	Gradual	0.1	75.0	*
26	photo-Fenton	Sulfuric	Gradual	0.2	75.0	*
27	photo-Fenton	Sulfuric	Gradual	0.4	75.0	*
28	photo-Fenton	Sulfuric	Gradual	0.8	75.0	*

\* Gradual additions of 250 mg H<sub>2</sub>O<sub>2</sub> at times 0, 60, 120 e 180 min, totaling 1000 mg

Synthetic wastewater was prepared with different indigo concentrations to study the influence of the initial dye concentration. The Fe<sup>2+</sup> concentration was kept stable (experiments 11 to 14) for Fenton and (experiments 25 to 28) for photo-Fenton. In these same solutions, the effect of the dosage of hydrogen peroxide was evaluated, where gradual additions of 250 mg of H<sub>2</sub>O<sub>2</sub> were carried out at times 0, 60, 120, and 180 minutes, totaling 1000 mg of H<sub>2</sub>O<sub>2</sub> added.

For both processes, 5 mL of treated wastewater samples were collected at time intervals of 0, 60, 120, 180, 240, 300, 360, 400, 420, and 480 minutes. To eliminate residual H<sub>2</sub>O<sub>2</sub> remaining in the solutions were added 0.15 mL catalase enzyme.

All collected samples were diluted 1:8 with distilled water, except for experiments 14 and 28, which were diluted 1:20 before analyzes in the UV/Vis spectrophotometer.



From the treated wastewater solutions, the concentration of remaining indigo, the color removal was determined, and the studies of the kinetic parameters were conducted according to items 2.4.1 to 2.4.3.

## 2.4 CALCULATIONS

### 2.4.1 Indigo concentrations remaining in the synthetic wastewater

To determine the maximum dye absorption peak, a 200-800 nm scan was performed for an indigo dye solution at  $0.2 \text{ g L}^{-1}$  using the Ultrospec 1100 pro UV visible spectrophotometer, equipment available in the Textile Research Laboratory Technicians - School of Arts, Sciences and Humanities, University of São Paulo. From the maximum absorbance wavelength of 664 nm, the standard curve was prepared at concentrations of 0.004, 0.008, 0.01, 0.02, 0.028, and  $0.04 \text{ g L}^{-1}$ , whose equation for the line was  $y = 0.0382x + 0.0019$  with  $R^2 = 0.9978$ . The calculation helped to determine the indigo concentrations remaining in the synthetic wastewater solutions at each time interval measured after the treatments by Fenton and photo-Fenton.

### 2.4.2 Removal efficiency

The color removal efficiency in the oxidation processes studied was calculated according to Eq. (11):

$$\text{Color Removal (\%)} = \frac{A_{\text{initial}} - A_{\text{final}}}{A_{\text{initial}}} \times 100 \quad (11)$$

where  $A_{\text{initial}}$  = initial absorbance e  $A_{\text{final}}$  = final absorbance.

Absorbance readings for each aliquot were taken in triplicate and the mean was calculated.

The maximum percentage of color removal in each process was considered as the average between the removal values obtained in each time interval in which the color removal curve showed stability.

### 2.4.3 Kinetic parameters

The kinetic calculation was performed based on zero-order, 1st, and 2nd order models, and the model developed by (Chan and Chu, 2003) specifically for the Fenton process and later used by (Behnajady, Modirshahla and Ghanbary, 2007), which was called BMG, an acronym formed by the initials of the study authors. The linearized equations of these models are presented in Eq. (12-15).

$$C_t = C_0 - k_0 \cdot t \quad (12)$$

$$\ln C_t = \ln C_0 - k_1 \cdot t \quad (13)$$

$$\frac{1}{C_t} = \frac{1}{C_0} + k_2 \cdot t \quad (14)$$

$$\frac{t}{[1-(C_t/C_0)]} = m + b \cdot t \quad (15)$$

Where  $k_0$ ,  $k_1$  and  $k_2$  are the zero-order, 1st and 2nd order kinetic constants, respectively;  $C_0$  is the initial dye concentration;  $C_t$  is the dye concentration at a given time, and  $t$  is the time.

As shown by (Chan and Chu, 2003; Behnajady, Modirshahla and Ghanbary, 2007), a graph formed from  $t/(1 - C_t/C_0)$  by  $t$  for the BMG model, results in a linearization with an intersection in  $m$  and a slope  $b$  (Santana et al., 2019; Nicodemos Ramos, Sousa and Aguiar, 2020). Thus, it can be concluded that the  $1/m$  parameter is related to the initial dye degradation rate and the  $1/b$  parameter is related to the maximum oxidation capacity of Fenton reactions (Santana et al., 2019).

### 3 RESULTS AND DISCUSSION

#### 3.1 COLOR REMOVAL EFFICIENCY

Wastewater treated by Fenton and Photo Fenton were evaluated by UV visible spectroscopy, and the absorbance values found were used to calculate the color removal efficiency. Dye concentrations were calculated from the calibration curves for each dye and the dye decolorization efficiency (%) was calculated using eq. (11) section 2.4.

When Fig. 3 is analyzed, the use of sulfuric acid for pH adjustment was more efficient for color removal than citric acid. The experiments with hydrogen peroxide ( $H_2O_2$ ) and ferrous iron ( $Fe^{2+}$ ) concentrations of  $1500 \text{ mg L}^{-1}$  and  $75 \text{ mg L}^{-1}$  respectively showed higher color removal efficiencies for both sulfuric acid (Exp. 5) and citric acid (Exp. 10). However, when sulfuric acid was used, the average color removal efficiency obtained was  $70.78 \pm 2.96 \%$  after 180 min and  $31.90 \pm 2.99 \%$  after 20 min using citric acid. In this case, it was observed a color removal of 54.93 % higher when sulfuric acid was used.

Fig. 3. Color removal of synthetic wastewater by the Fenton process using (a) sulfuric acid and (b) citric acid, to pH 2.8 adjust

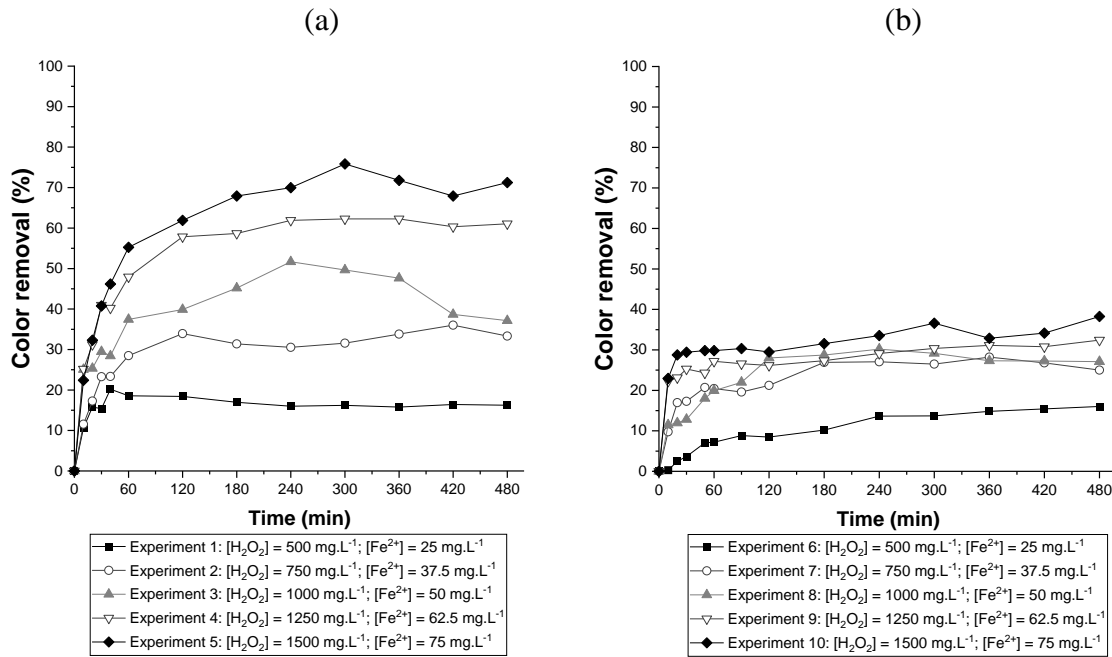
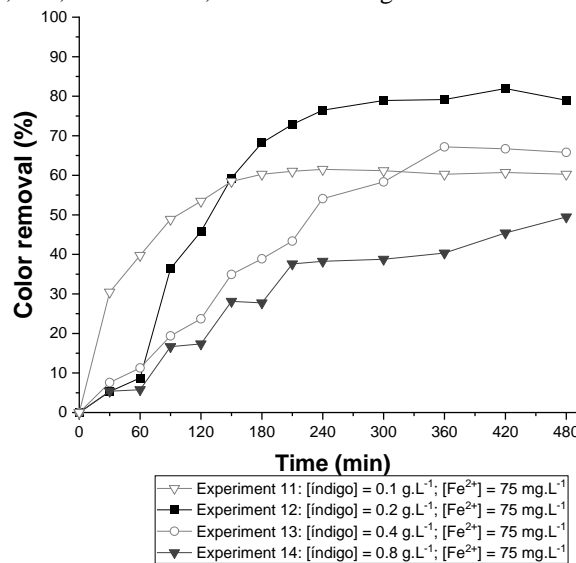
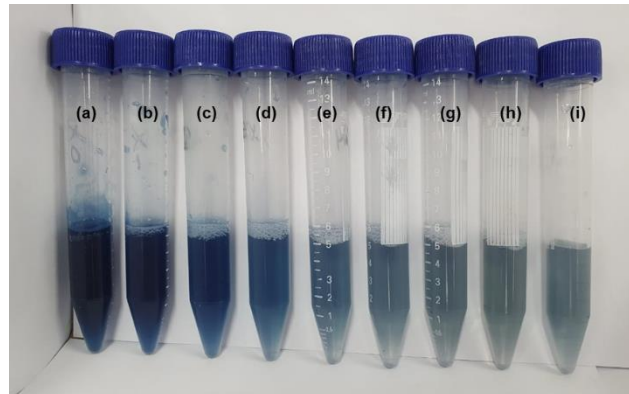


Fig. 4. Color removal of synthetic wastewater by Fenton using sulfuric acid to pH 2.8 adjust and gradual addition of 250 mg of H<sub>2</sub>O<sub>2</sub> at times 0, 60, 120, and 180 min, to total 1000 mg of H<sub>2</sub>O<sub>2</sub>



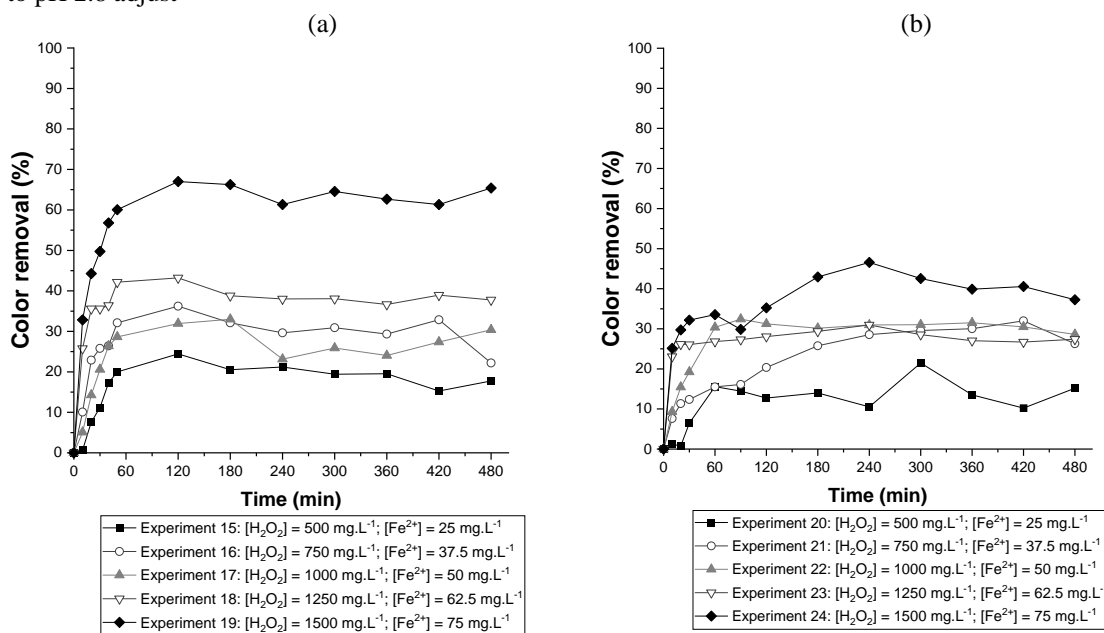
In Fig. 4 the color removal results of the experiments carried out with the gradual addition of H<sub>2</sub>O<sub>2</sub> are shown. The synthetic wastewater with a concentration of 0.2 g L<sup>-1</sup> indigo and 75 mg L<sup>-1</sup> of Fe<sup>2+</sup> (Exp. 12) achieved an average color removal of 79.76 ± 1.46 % after 300 min. This color removal efficiency value was the best result for the Fenton process with the gradual addition of H<sub>2</sub>O<sub>2</sub>. And the color removal can be observed in the collected samples showed in Fig. 5.

Fig. 5. Falcon tubes containing aliquots taken from sample 12 during the Fenton process with the gradual addition of H<sub>2</sub>O<sub>2</sub>. a) = 0 min; (b) = 60 min; (c) = 120 min; (d) = 180 min; (e) = 240 min; (f) = 300 min; (g) = 360 min; (h) = 420 min; (i) = 480 min.



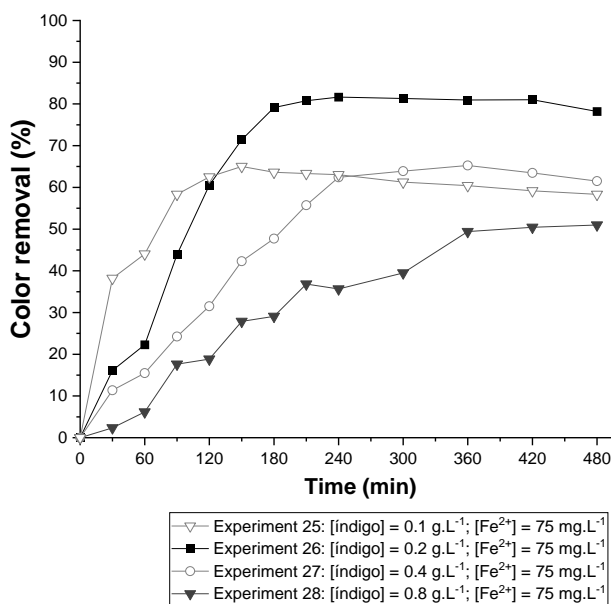
For the photo-Fenton process (Fig. 6), the hydrogen peroxide (H<sub>2</sub>O<sub>2</sub>) and ferrous iron (Fe<sup>2+</sup>) concentration of 1500 mg L<sup>-1</sup> and 75 mg L<sup>-1</sup> respectively, the maximum color removals to sulfuric acid and citric acid obtained were 64.22 ± 2.08 % after 60 min (Exp. 19) and 41.62 ± 3.17 % after 180 min (Exp. 24).

Fig. 6. Color removal of synthetic wastewater by the photo-Fenton process using (a) sulfuric acid and (b) citric acid, to pH 2.8 adjust



The color removal by photo-Fenton that experiments with the gradual addition of H<sub>2</sub>O<sub>2</sub> is shown in Fig. 7. The highest removal efficiency observed in these experiments was 80.42 ± 1.27 % after 180 min with indigo and Fe<sup>2+</sup> concentration of 0.2 g L<sup>-1</sup> and 75 mg L<sup>-1</sup> (Exp. 26).

Fig. 7. Color removal of synthetic wastewater by photo-Fenton using sulfuric acid to pH 2.8 adjust and gradual addition of 250 mg of H<sub>2</sub>O<sub>2</sub> at times 0, 60, 120, and 180 min, to total 1000 mg of H<sub>2</sub>O<sub>2</sub>



A summary of the best results obtained by Fenton and photo-Fenton processes are showed in Table 2

Table 2. Experiments with the best color removal efficiency results by Fenton and photo-Fenton processes in the treatment of synthetic effluents containing indigo dye

Experiments	Method	Acid	H <sub>2</sub> O <sub>2</sub> Dosage	Color Removal (%)	Time (min)
5	Fenton	Sulfuric	Single	70.78 ± 2.96	180
12	Fenton	Sulfuric	Gradual	79.76 ± 1.46	300
19	photo-Fenton	Sulfuric	Single	64.22 ± 2.08	60
26	photo-Fenton	Sulfuric	Gradual	80.43 ± 1.27	180

In general, the best results for the advanced oxidation processes analyzed were using sulfuric acid to pH adjustment (Table 2). It can be explained by citric acid to be considered a weak organic acid, while sulfuric acid is classified as a strong inorganic acid. Therefore, higher concentrations of citric acid are needed to reach the same pH value with the use of sulfuric acid (Toratane, 2013). Furthermore, the solution's citric acid can compete with the indigo dye molecules, and it can be degraded by the attack of •OH hydroxyl radicals since •OH is a non-selective radical (Huang et al., 2018).

In addition, the degradation of organic molecules by •OH can lead to the formation of carboxylic acids, such as citric acid, which interferes with the balance of the Fenton reaction, decreasing the generation of •OH radicals and, consequently, a decrease in the efficiency of color removal (Baba et al., 2015).

Photo-Fenton was expected to be more efficient in the treatment of wastewaters, as it produces greater amounts of  $\bullet\text{OH}$ , which can enhance the efficiency of degradation of organic pollutants (Zhang et al., 2019). However, in this work, the color removal ability was not increased by ultraviolet light irradiation (photo-Fenton). Although higher color removal percentages were not observed in photo-Fenton processes compared to Fenton, with a single dose of  $\text{H}_2\text{O}_2$ , it was noted that the maximum removal efficiencies occurred in shorter time intervals.

This may be related to the fact that the prepared solutions have a relatively high dye concentration, increasing turbidity, making it difficult for UV light to penetrate the solution and, consequently, for absorbing UV light necessary for the photo-Fenton reaction, hindering the generation of  $\bullet\text{OH}$  radicals (Mirzaei et al., 2017).

Considering the increased concentration of  $\text{H}_2\text{O}_2$  and  $\text{Fe}^{2+}$  (Fig. 3 and 6), the best color removal efficiencies were obtained. That can be explained by the increase of hydroxyl  $\bullet\text{OH}$  radicals' production, which are responsible for rapidly degrading the dye molecules. However, excessive concentrations of  $\text{Fe}^{2+}$  can decrease the removal efficiency due to the elimination of  $\bullet\text{OH}$  by  $\text{Fe}^{2+}$  (Eq. 7) (Zhang et al., 2019). And excessive concentrations of  $\text{H}_2\text{O}_2$  should also be avoided, as high concentrations of  $\text{H}_2\text{O}_2$  can increase the  $\bullet\text{OH}$  scavenging effect (Eq. 6) (Mirzaei et al., 2017).

The effect of high concentrations of indigo on color removal efficiencies could be observed. The initial dye concentration was progressively doubled in Exp. 11 to 14 for the Fenton process and Exp. 25 to 28 for the photo-Fenton process.

According to the results presented in Figs. 4 and 7, it can be noted that the higher the initial dye concentration, the greater the amount of degraded dye, if the percentage of color removal is considered as the reduction of the initial amount of dye present in each experiment.

Thus, it can be observed that the relationship between the amount of  $\text{Fe}^{2+}$  and  $\text{H}_2\text{O}_2$  depends directly on the initial amount of dye so that treatments by improved the efficient in color removal (Zhang et al., 2019). Therefore, the higher the initial concentration of indigo dye present in the solution, the greater the amount of dye molecules that were attacked by  $\bullet\text{OH}$  radicals generated in the Fenton and photo-Fenton (i.e. more dye molecules in the solution greater is the possibility of collision with the  $\bullet\text{OH}$  radical). However, the increase in the initial concentration of the dye could not result in higher percentages of color removal (Mirzaei et al., 2017).

In this work, the highest color removal efficiencies were obtained when  $\text{H}_2\text{O}_2$  was feeding in multiple stages (Table 2). An increase of 8.98% was observed for the Fenton process (Exp. 12) and 16.21% for photo-Fenton (Exp. 26) with the gradual addition of  $\text{H}_2\text{O}_2$  to the treatments with single-step addition. The initial proportion in which hydrogen peroxide is added to the

synthetic effluent solution can alter the reaction mechanism, significantly increase the color removal efficiency, and, consequently, the dye degradation. Radical  $\bullet\text{OH}$  has a very short lifetime and it can be eliminated from the reaction at higher concentrations of  $\text{H}_2\text{O}_2$  (Yu et al., 2020).

In addition,  $\bullet\text{OH}$  competes with other species that participate in Fenton and photo-Fenton reactions, such as iron ions, other generated radicals, the dye, and its intermediates produced (Ebrahiem, Al-Maghrabi and Mobarki, 2017; Zúñiga-Benítez, Muñoz-Calderón and Peñuela, 2018).

Therefore, the gradual addition of  $\text{H}_2\text{O}_2$  maintains its concentration relatively low, decreasing the  $\bullet\text{OH}$  radical scavenging and consequently, increasing the possibility of collision with the dye molecule (Hafezi et al., 2020; Yu et al., 2020).

### 3.2 Kinetic Parameters determination

Linear regression analyzes of zero-order, 1st, and 2nd order reaction kinetics for the synthetic effluent solutions tested by Fenton and photo-Fenton were conducted. The values of  $k_0$ ,  $k_1$ , and  $k_2$ , and the kinetic parameters of the BMG model,  $1/m$  and  $1/b$ , were also obtained (Table 3).

A correlation coefficient ( $R^2$ ) value close to 1 was considered as a better fit of the experimental data to the kinetic models. As observed in Table 3, the BMG model was better fitting for the advanced oxidation processes tested, as it obtained  $R^2$  values closer to 1 than the zero-order, 1st, and 2nd order kinetic models (Nicodemos Ramos, Sousa and Aguiar, 2020).

Fenton's process, using  $\text{Fe}^{2+}$  as a catalyst for the oxidation reaction, ordinarily occurs through two steps, one fast and the other slower. The first fast stage is related to the reaction between  $\text{Fe}^{2+}$  and  $\text{H}_2\text{O}_2$  (Eq. 1) and the slower stage to the accumulation of  $\text{Fe}^{3+}$  and low recovery of  $\text{Fe}^{2+}$  due to  $\text{H}_2\text{O}_2$  (Santana et al., 2019). In addition, the reaction of  $\text{Fe}^{3+}$  with  $\text{H}_2\text{O}_2$  (Eq. 2) reduces the concentration of  $\text{H}_2\text{O}_2$  in the solution in the solution and the formation of the  $\text{HO}_2\bullet$  radical, which has a low oxidation potential (Santana et al., 2019). Ramos, Souza and Aguiar (2020) observed the same performance for the degradation of different dyes through the Fenton process using cysteine and its effects on the activation energy.

The reactions of  $\text{Fe}^{2+}/\text{H}_2\text{O}_2$  with the indigo dye showed a two-stage pattern. However, the Fenton reaction with indigo dye could not be modeled by zero-order, first, or second-order reaction kinetics. Therefore, the most adequate system kinetics to represent the Fenton process was the BMG model.

Table 3. Kinetic rate constants of the zero ( $k_0$ ), 1st ( $k_1$ ), and 2nd order ( $k_2$ ), parameters obtained on the BMG model ( $1/m$  and  $1/b$ ), and correlation coefficients ( $R^2$ ) obtained for the Fenton and photo-Fenton process.

Experiments	Zero-order		First Order		Second Order		BMG		
	$k_0$ ( $\text{g L}^{-1} \text{min}^{-1}$ )	$R^2$	$k_1$ ( $\text{min}^{-1}$ )	$R^2$	$k_2$ ( $\text{L g}^{-1} \text{min}^{-1}$ )	$R^2$	$1/m$ ( $\text{min}^{-1}$ )	$1/b$	$R^2$
1	$-1.46 \times 10^{-5}$	0.0921	$-8.97 \times 10^{-5}$	0.0861	$-5.52 \times 10^{-4}$	0.0799	-0.0418	0.1450	0.9985
2	$-8.49 \times 10^{-5}$	0.5222	$-5.87 \times 10^{-4}$	0.5664	0.0041	0.6104	0.0187	0.3200	0.9928
3	$-2.25 \times 10^{-4}$	0.6058	-0.0013	0.6891	0.0073	0.7552	0.0256	0.4792	0.9908
4	$-1.47 \times 10^{-4}$	0.5000	-0.0012	0.5865	0.0106	0.6587	0.0419	0.5815	0.9983
5	$-2.42 \times 10^{-4}$	0.5423	-0.0019	0.6671	0.0161	0.7676	0.0345	0.6956	0.9978
6	$-4.56 \times 10^{-5}$	0.8634	$-2.93 \times 10^{-4}$	0.8762	0.0019	0.8883	0.0018	0.1665	0.9562
7	$-6.83 \times 10^{-5}$	0.5683	$-4.62 \times 10^{-4}$	0.6039	0.0031	0.6379	0.0161	0.2558	0.9950
8	$-6.78 \times 10^{-5}$	0.5325	$-4.43 \times 10^{-4}$	0.5482	0.0029	0.5607	0.0149	0.2633	0.9911
9	$-5.08 \times 10^{-5}$	0.3867	$-3.45 \times 10^{-4}$	0.4341	0.0024	0.4844	0.0294	0.2886	0.9969
10	$-6.69 \times 10^{-5}$	0.3451	$-4.66 \times 10^{-4}$	0.4058	0.0033	0.4720	0.0261	0.3449	0.9935
15	$-2.60 \times 10^{-5}$	0.1804	$-1.69 \times 10^{-4}$	0.1719	0.0011	0.1626	-0.0354	0.1591	0.9683
16	$-5.61 \times 10^{-5}$	0.2590	$-3.84 \times 10^{-4}$	0.2707	0.0027	0.2816	0.0470	0.2868	0.9939
17	$-5.66 \times 10^{-5}$	0.2518	$-3.52 \times 10^{-4}$	0.2546	0.0022	0.2559	0.0257	0.2694	0.9835
18	$-4.69 \times 10^{-5}$	0.0952	$-2.42 \times 10^{-4}$	0.0818	0.0012	0.0662	-0.0826	0.3485	0.9979
19	$-1.56 \times 10^{-4}$	0.2675	-0.0011	0.3178	0.0077	0.3551	0.1324	0.6117	0.9987
20	$-3.03 \times 10^{-5}$	0.3338	$-2.01 \times 10^{-4}$	0.3353	0.0013	0.3366	0.0034	0.1396	0.9274
21	$-9.84 \times 10^{-5}$	0.8426	$-6.92 \times 10^{-4}$	0.8733	0.0049	0.8997	0.0063	0.3089	0.9803
22	$-9.67 \times 10^{-5}$	0.4884	$-6.52 \times 10^{-4}$	0.5153	0.0044	0.5404	0.0199	0.2978	0.9962
23	$-2.92 \times 10^{-5}$	0.1434	$-1.86 \times 10^{-4}$	0.1487	0.0012	0.1542	-0.2020	0.2474	0.9987
24	$-7.60 \times 10^{-5}$	0.3619	$-5.29 \times 10^{-4}$	0.3904	0.0038	0.4099	0.2590	0.3651	0.9895

Analyzing the kinetic parameters of the BMG model presented in Table 3, it can be observed that the values of  $1/b$  increased as the concentrations of  $\text{Fe}^{2+}$  and  $\text{H}_2\text{O}_2$  were higher in the experiments. Therefore, the higher the  $\text{Fe}^{2+}$  and  $\text{H}_2\text{O}_2$  concentration, the greater the dye's oxidation capacity and, consequently, greater color removal.

The Fenton process can be accelerated by UV light (photo Fenton) increasing the generation of the  $\bullet\text{OH}$  radical by  $\text{Fe}^{3+}$  reduction (Eq. 3) to more efficient contaminants degradation using fewer reagents concentration or lower reaction times (Ebrahiem, Al-Maghrabi and Mobarki, 2017). The highest values of  $1/m$  were obtained for the photo-Fenton experiments that contained the highest concentrations of  $\text{H}_2\text{O}_2$  and  $\text{Fe}^{2+}$  (Exp. 19 and 24) indicating that these



experiments had a higher initial removal rate compared to other experiments, as shown in Figs. 3 and 6.

The kinetic parameters of the zero-order, 1st and 2nd order, and the BMG model were not determined for the treatments with gradual addition of  $H_2O_2$ . That happens because each dosage of  $H_2O_2$  leads to a lower concentration of dye compared to the previous dosage and, as part of the dye has already suffered degradation, at each dosage of  $H_2O_2$  a different initial reaction rates occurs. In addition, the BMG kinetic model was developed through experiments conducted with a single dose of reagents (Chan and Chu, 2003; Behnajady, Modirshahla and Ghanbary, 2007).

#### 4 CONCLUSIONS

The present work studied the color removal efficiency by Fenton and photo-Fenton in a synthetic wastewater aqueous solution containing indigo blue obtaining values between 70 and 80 %. It was found that the parameters such as strong acid use, hydrogen peroxide gradual addition and increased concentration of  $H_2O_2$  and  $Fe^{2+}$  positively affected the color removal efficiencies for both processes studied. However, high concentrations of indigo in the synthetic wastewater caused a drop in efficiency values. UV light irradiation did not cause a significant improvement in color removal ability in the synthetic wastewater used in this work. The BMG model was a good adjustment to the color removal evaluating. Then, Fenton and photo-Fenton with parameters minutely adjusted could be used to textile wastewater containing indigo blue treatment.

#### ACKNOWLEDGMENTS

This research was conducted mainly in the Technical Textile Research Laboratory in the School of Arts, Sciences and Humanity, at the University of São Paulo. The authors thank Labtex Laboratory for the analysis support.

## REFERENCES

Amaral, M. C. S. et al. (2014) 'Evaluation of operational parameters from a microfiltration system for indigo blue dye recovery from textile dye effluent', *Desalination and Water Treatment*, 52(1–3), pp. 257–266. doi: 10.1080/19443994.2013.793618.

Ameta, R. et al. (2018) Fenton and Photo-Fenton Processes, *Advanced Oxidation Processes for Wastewater Treatment: Emerging Green Chemical Technology*. doi: 10.1016/B978-0-12-810499-6.00003-6.

Baba, Y. et al. (2015) 'Hydroxyl radical generation in the photo-fenton process: Effects of carboxylic acids on iron redox cycling', *Chemical Engineering Journal*. Elsevier B.V., 277, pp. 229–241. doi: 10.1016/j.cej.2015.04.103.

Babuponnusami, A. and Muthukumar, K. (2014) 'A review on Fenton and improvements to the Fenton process for wastewater treatment', *Journal of Environmental Chemical Engineering*. Elsevier Ltd, 2(1), pp. 557–572. doi: 10.1016/j.jece.2013.10.011.

Behnajady, M. A., Modirshahla, N. and Ghanbary, F. (2007) 'A kinetic model for the decolorization of C.I. Acid Yellow 23 by Fenton process', *Journal of Hazardous Materials*, 148(1–2), pp. 98–102. doi: 10.1016/j.jhazmat.2007.02.003.

Chan, K. H. and Chu, W. (2003) 'Modeling the reaction kinetics of Fenton's process on the removal of atrazine', *Chemosphere*, 51(4), pp. 305–311. doi: 10.1016/S0045-6535(02)00812-3.

Chowdhury, M. F. et al. (2020) 'Current treatment technologies and mechanisms for removal of indigo carmine dyes from wastewater: A review', *Journal of Molecular Liquids*. Elsevier B.V., 318, p. 114061. doi: 10.1016/j.molliq.2020.114061.

Dojčinović, B. P. et al. (2011) 'Decolorization of reactive textile dyes using water falling film dielectric barrier discharge', *Journal of Hazardous Materials*, 192(2), pp. 763–771. doi: 10.1016/j.jhazmat.2011.05.086.

Ebrahiem, E. E., Al-Maghrabi, M. N. and Mobarki, A. R. (2017) 'Removal of organic pollutants from industrial wastewater by applying photo-Fenton oxidation technology', *Arabian Journal of Chemistry*. King Saud University, 10, pp. S1674–S1679. doi: 10.1016/j.arabjc.2013.06.012.

Garcia, B. (2015) *Reduced water washing of denim garments*, *Denim: Manufacture, Finishing and Applications*. Elsevier Ltd. doi: 10.1016/B978-0-85709-843-6.00013-5.

Garcia, L. F. et al. (2017) 'Bio-electro oxidation of indigo carmine by using microporous activated carbon fiber felt as anode and bioreactor support', *Chemosphere*, 186, pp. 519–526. doi: 10.1016/j.chemosphere.2017.08.033.

Ghazi Mokri, H. S. et al. (2015) 'Adsorption of C.I. Acid Red 97 dye from aqueous solution onto walnut shell: kinetics, thermodynamics parameters, isotherms', *International Journal of Environmental Science and Technology*, 12(4), pp. 1401–1408. doi: 10.1007/s13762-014-0725-6.

Hafezi, M. et al. (2020) 'Application of impinging jet atomization in UV/H<sub>2</sub>O<sub>2</sub> reactor operation: Design, evaluation, and optimization', *Journal of Photochemistry and Photobiology A: Chemistry*, 389(June 2019). doi: 10.1016/j.jphotochem.2019.112198.

Hendaoui, K. et al. (2018) 'Real indigo dyeing effluent decontamination using continuous electrocoagulation cell: Study and optimization using Response Surface Methodology', *Process Safety and Environmental Protection*. Institution of Chemical Engineers, 116, pp. 578–589. doi: 10.1016/j.psep.2018.03.007.

Huang, T. et al. (2018) 'Fe<sup>0</sup>-H<sub>2</sub>O<sub>2</sub> for advanced treatment of citric acid wastewater: Detailed study of catalyst after several times use', *Chemical Engineering Journal*. Elsevier, 336(August 2017), pp. 233–240. doi: 10.1016/j.cej.2017.11.147.

Kalra, A. and Gupta, A. (2019) 'Recent advances in decolourization of dyes using iron nanoparticles: A mini review', *Materials Today: Proceedings*. Elsevier Ltd., 36, pp. 689–696. doi: 10.1016/j.matpr.2020.04.677.

Katheresan, V., Kansedo, J. and Lau, S. Y. (2018) 'Efficiency of various recent wastewater dye removal methods: A review', *Journal of Environmental Chemical Engineering*, 6(4), pp. 4676–4697. doi: 10.1016/j.jece.2018.06.060.

Khatri, I., Singh, S. and Garg, A. (2018) 'Performance of electro-Fenton process for phenol removal using Iron electrodes and activated carbon', *Journal of Environmental Chemical Engineering*. Elsevier, 6(6), pp. 7368–7376. doi: 10.1016/j.jece.2018.08.022.

Kumar, V., Singh, K. and Shah, M. . (2021) 'Advanced oxidation processes for complex wastewater treatment', in Shah, M. . (ed.) *Advanced Oxidation Processes for Effluent Treatment Plants*. Cambridge, pp. 1–31.

Lima, J. P. P. et al. (2021) 'Kinetic Evaluation of Bismarck Brown Y Azo Dye Oxidation by Fenton Processes in the Presence of Aromatic Mediators', *Water, Air, and Soil Pollution*. Springer International Publishing, 232(8). doi: 10.1007/s11270-021-05258-1.

Mahakulkar, S. et al. (2019) 'Advanced Oxidative Degradation of Indigo Carmine', *International Journal of Innovations in Engineering and Science*, 4(8), pp. 225–228.

Mahtab, M. S., Farooqi, I. H. and Khurshed, A. (2021) 'Sustainable approaches to the Fenton process for wastewater treatment: A review', *Materials Today: Proceedings*. Elsevier Ltd, (xxxx). doi: 10.1016/j.matpr.2021.04.215.

Meksi, N. and Mhenni, M. F. (2015) *Indigo dyeing technology for denim yarns, Denim: Manufacture, Finishing and Applications*. Elsevier Ltd. doi: 10.1016/B978-0-85709-843-6.00004-4.

Miller, C. J., Wadley, S. and Waite, T. D. (2017) 'Fenton, photo-Fenton and Fenton-like processes', *Water Intelligence Online*, 16, pp. 297–332. doi: 10.2166/9781780407197\_0297.

Mirzaei, A. et al. (2017) 'Removal of pharmaceuticals from water by homo/heterogeneous Fenton-type processes – A review', *Chemosphere*. Elsevier Ltd, 174, pp. 665–688. doi: 10.1016/j.chemosphere.2017.02.019.

Mishra, N. et al. (2017) 'A Review on Advanced Oxidation Processes for Effective Water Treatment', *Current World Environment*, 12(3), pp. 469–489. doi: 10.12944/CWE.12.3.02.

Nature (2021) In the jeans: an environmentally friendly way to dye denim could usher in a long-overdue new fashion. Available at: <https://media.nature.com/original/magazine-assets/d41586-018-00103-8/d41586-018-00103-8.pdf> (Accessed: 21 July 2021).

Nicodemos Ramos, M. D., Sousa, L. A. and Aguiar, A. (2020) 'Effect of cysteine using Fenton processes on decolorizing different dyes: a kinetic study', *Environmental Technology* (United Kingdom). Taylor & Francis, 0(0), pp. 1–13. doi: 10.1080/09593330.2020.1776402.

Ou, X. et al. (2013) 'Degradation of methyl violet by Fenton's reagent: Kinetic modeling and effects of parameters', *Desalination and Water Treatment*, 51(13–15), pp. 2536–2542. doi: 10.1080/19443994.2012.749000.

Palma-Goyes, R. E. et al. (2014) 'Comparative degradation of indigo carmine by electrochemical oxidation and advanced oxidation processes', *Electrochimica Acta*. Elsevier Ltd, 140, pp. 427–433. doi: 10.1016/j.electacta.2014.06.096.

Palma-Goyes, R. E. et al. (2018) 'The effect of different operational parameters on the electrooxidation of indigo carmine on Ti/IrO<sub>2</sub>-SnO<sub>2</sub>-Sb<sub>2</sub>O<sub>3</sub>', *Journal of Environmental Chemical Engineering*, 6(2), pp. 3010–3017. doi: 10.1016/j.jece.2018.04.035.

Paul, R. (2015) *Denim and jeans: An overview*, Denim: Manufacture, Finishing and Applications. Elsevier Ltd. doi: 10.1016/B978-0-85709-843-6.00001-9.

Qiu, M. and Huang, C. (2010) 'A comparative study of degradation of the azo dye C.I. Acid Blue 9 by Fenton and photo-Fenton oxidation', *Desalination and Water Treatment*, 24(1–3), pp. 273–277. doi: 10.5004/dwt.2010.1619.

Ramos, M. D. N. et al. (2021) 'A critical analysis of the alternative treatments applied to effluents from Brazilian textile industries', *Journal of Water Process Engineering*, 43(May), p. 102273. doi: 10.1016/j.jwpe.2021.102273.

Ramos, R. O. et al. (2020) 'Degradation of indigo carmine by photo-Fenton, Fenton, H<sub>2</sub>O<sub>2</sub>/UV-C and direct UV-C: Comparison of pathways, products and kinetics', *Journal of Water Process Engineering*. Elsevier, 37(May), p. 101535. doi: 10.1016/j.jwpe.2020.101535.

Saggiaro, E. M. et al. (2015) 'Photo-decolorization and ecotoxicological effects of solar compound parabolic collector pilot plant and artificial light photocatalysis of indigo carmine dye', *Dyes and Pigments*, 113, pp. 571–580. doi: 10.1016/j.dyepig.2014.09.029.

Santana, C. S. et al. (2019) 'Kinetic evaluation of dye decolorization by fenton processes in the presence of 3-hydroxyanthranilic acid', *International Journal of Environmental Research and Public Health*, 16(9). doi: 10.3390/ijerph16091602.

Toratane, M. (2013) 'Where is the Border Line between Strong Acids and Weak Acids?', *World Journal of Chemical Education*, 1(1), pp. 12–16. doi: 10.12691/wjce-1-1-4.

Vedrenne, M. et al. (2012) 'A ferrous oxalate mediated photo-Fenton system: Toward an

increased biodegradability of indigo dyed wastewaters', *Journal of Hazardous Materials*. Elsevier B.V., 243, pp. 292–301. doi: 10.1016/j.jhazmat.2012.10.032.

Yu, X. et al. (2020) 'An experimental approach to the optimization of the dosage of hydrogen peroxide for Fenton and photo-Fenton processes', *Science of the Total Environment*, 743. doi: 10.1016/j.scitotenv.2020.140402.

Yukseler, H. et al. (2017) 'Analysis of the best available techniques for wastewaters from a denim manufacturing textile mill', *Journal of Environmental Management*. Elsevier Ltd, 203, pp. 1118–1125. doi: 10.1016/j.jenvman.2017.03.041.

Zhang, M. hui et al. (2019) 'A review on Fenton process for organic wastewater treatment based on optimization perspective', *Science of the Total Environment*. Elsevier B.V., 670, pp. 110–121. doi: 10.1016/j.scitotenv.2019.03.180.

Zhao, Z. et al. (2020) 'Degradation of indigo carmine by coupling Fe(II)-activated sodium persulfate and ozone in a rotor-stator reactor', *Chemical Engineering and Processing - Process Intensification*. Elsevier, 148(June 2019), p. 107791. doi: 10.1016/j.cep.2019.107791.

Zukawa, T. et al. (2019) 'Photolysis of Indigo Carmine solution by planar vacuum-ultraviolet (147 nm) light source', *Chemosphere*. Elsevier Ltd, 214, pp. 123–129. doi: 10.1016/j.chemosphere.2018.09.102.

Zúñiga-Benítez, H., Muñoz-Calderón, A. and Peñuela, G. A. (2018) 'Removal of a mix of benzophenones and parabens using solar photo-Fenton and a cylinder parabolic collector in aqueous solutions', *Journal of Environmental Chemical Engineering*. Elsevier, 6(6), pp. 7347–7357. doi: 10.1016/j.jece.2018.08.039.